JOC Article

Kinetics and Mechanism of the Cleavage of Phthalic Anhydride in Glacial Acetic Acid Solvent Containing Aniline

Emmy Fadhiza Damit, Azhar Ariffin, and M. Niyaz Khan*

Department of Chemistry, Faculty of Science, University of Malaya, 50603 Kuala Lumpur, Malaysia

niyaz@um.edu.my

Received May 22, 2008

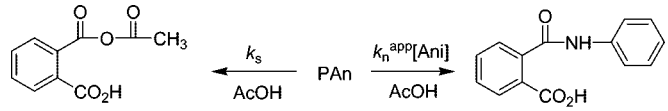

AcOH = glacial acetic acid
PAn = phthalic anhydride
Ani = aniline

Apparent second-order rate constants (k_n^{app}) for the nucleophilic reaction of aniline (Ani) with phthalic anhydride (PAn) vary from 6.30 to 7.56 M^{-1} s^{-1} with the increase of temperature from 30 to 50 °C in pure glacial acetic acid (AcOH). However, the values of pseudo-first-order rate constants (k_s) for the acetolysis of PAn in pure AcOH increase from 16.5 × 10^{-4} to 10.7 × 10^{-3} s^{-1} with the increase of temperature from 30 to 50 °C. The values of k_n^{app} and k_s vary from 5.84 to 7.56 M^{-1} s^{-1} and from 35.1 × 10^{-4} to 12.4 × 10^{-4} s^{-1}, respectively, with the increase of CH_3CN content from 1% to 80% v/v in mixed AcOH solvents at 35 °C. The plot of k_s versus CH_3CN content shows a minimum (with 10^4 k_s = 4.40 s^{-1}) at 50% v/v CH_3CN. Similarly, the variations of k_n^{app} and k_s with the increasing content of tetrahydrofuran (THF) in mixed AcOH solvent reveal respective a maximum (with k_n^{app} = 17.5−15.6 M^{-1} s^{-1}) at 40−60% v/v THF and a minimum (with k_s = ∼ 0−1.2 × 10^{-4} s^{-1}) at 60−70% v/v THF. The respective values of ΔH^* and ΔS^* are 15.3 ± 1.2 kcal mol^{-1} and −20.1 ± 3.8 cal K^{-1} mol^{-1} for k_s and 1.1 ± 0.5 kcal mol^{-1} and −51.2 ± 1.7 cal K^{-1} mol^{-1} for k_n^{app}, while the values of k_n (= k_n^{app}/f_b with f_b representing the fraction of free aniline base) are almost independent of temperature within the range 30−50 °C. A spectrophotometric approach has been described to determine f_b in AcOH as well as mixed AcOH−CH_3CN and AcOH−THF solvents. Thus, the observed data, obtained under different reaction conditions, have been explained quantitatively. An optimum reaction condition, within the domain of present reaction conditions, has been suggested for the maximum yield of the desired product, *N*-phenylphthalamic acid.

Introduction

Diagnosis of fine molecular details of mechanisms of reactions carried out in mixed aqueous−organic cosolvents and pure organic solvents is complicated by the uncertainty of the measurements of pH of buffers and pK_a or pK_b of acids or bases in such solvents. Partly because of this and related reasons, very limited reports could be found in this area of research.[1] However, organic and mixed organic solvents are generally the best reaction solvents for the synthesis of organic compounds. The kinetic study provides the mechanistic details of a reaction at the molecular level and hence such kinetic studies in organic and mixed organic solvents are expected to give the optimum reaction conditions for maximum yields of the desired organic products. Recently, Perry and Parveen[2] carried out a systematic kinetic study of the cyclization of substituted phthalanilic acids to *N*-arylphthalimide derivatives in glacial acetic acid solution. These authors have provided mechanistic details of these reaction processes where kinetic and ^1H NMR spectrometric evidence have been presented for the presence of reactive intermediate (**1**) on the reaction path. Perhaps it is important to note that the intermediate similar to **1** could not be detected in several studies on the cleavage of phthalanilic and substituted phthalanilic acids in pure and mixed acidic aqueous−organic cosolvents.[3−6] *N*-Alkyl and *N*-arylphthalimides have been conveniently synthesized in good yield by heating or refluxing

(1) Godenschwager, P. F.; Collum, D. B. *J. Am. Chem. Soc.* **2007**, *129*, 12023, and references therein.

(2) Perry, C. J.; Parveen, Z. *J. Chem. Soc., Perkin Trans.* **2001**, *2*, 512.

(3) Hawkins, D. M. *J. Chem. Soc., Perkin Trans.* **1976**, *2*, 642.

10.1021/jo8011072 CCC: $40.75 © 2008 American Chemical Society
Published on Web 10/28/2008

SCHEME 1

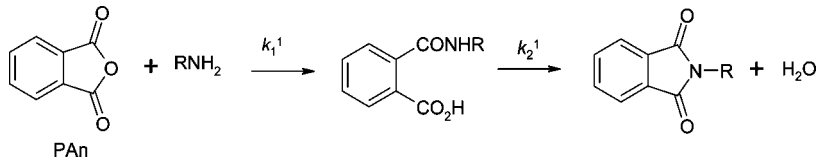

the reaction mixture of phthalic anhydride and alkyl or arylamine in glacial acetic acid.[7] In view of the published related studies, the expected reaction scheme for the formation of *N*-substituted phthalimide from the reaction of phthalic anhydride (PAn) with a primary amine, RNH_2, in acidic solution is shown by Scheme 1. Mechanistic details of the k_2^1-step for the cleavage of *N*-phenylphthalamic acid in glacial acetic acid at 85 °C are already reported.[2]

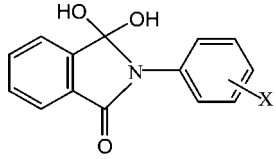

1

The present study was initiated with the aims (i) to find an experimental approach to determine the fraction of free amine base (f_b) in nonaqueous solvents where conventional technique involving pH measurements becomes unable to provide such information (i.e., f_b), (ii) to find the mechanistic details of the reaction of phthalic anhydride with aniline in glacial acetic acid solution (i.e., k_2^1-step of scheme 1), and (iii) to determine an optimum condition for maximum yield of product *N*-phenylphthalamic acid. The observed data and their plausible explanation(s) are described in this manuscript.

Results

Effects of [Aniline] on the Cleavage of Phthalic Anhydride (PAn) in Glacial Acetic Acid Solution. Several runs were carried within the total aniline concentration $[Ani]_T$, range 5.0 $\times$ 10^{-4} - 4.0 $\times$ 10^{-3} M at a constant temperature in glacial acetic acid solution containing 1.5 $\times$ 10^{-4} M phthalic anhydride. Pseudofirst-order rate constant (k_{obs}) are shown graphically (Figure 1) at different temperatures ranging from 30 to 50 °C. The values of k_{obs} at different $[Ani]_T$ and at a constant temperature were found to fit to eq 1

$$k_{obs} = k_s + k_n^{app}[Ani]_T \quad (1)$$

where k_s and k_n^{app} represent respective pseudo-first-order rate constant for solvent-assisted and second-order rate constant for aniline-assisted cleavage of PAn. The least-squares calculated values of k_s and k_n^{app} at different temperature are summarized in Table 1. the reliability of the observed data fit to eq 1 is evident from the standard deviations associated with k_s and k_n^{app} values (Table 1) and from the plots of Figure 1 where the solid lines are drawn through the least-squares calculated data points using eq 1 and kinetic parameters, k_s and k_n^{app}, listed in Table 1.

It is evident from eq 1 as well as product characterization study that a brief reaction scheme for the cleavage of PAn in glacial acetic acid containing Ani may be expressed by Scheme 2 where PAn and Ani represent phthalic anhydride and nonprotonated aniline, respectively.

Determination of Fraction of Free Aniline Base (f_b) in Glacial Acetic Acid Solution. It is practically almost impossible to determine accurately the pK_a of an acid such as anilinium in an organic solvent (such as glacial acidic acid) of dielectric constant (ε) ~6.[8] Under such circumstances, a quantitative interpretation of kinetic data of Figure 1 is apparently difficult to achieve. The linearity of the plots of Figure 1 shows that the fraction of free base, $[Ani]/[Ani]_T$, (where Ani represents nonprotonated aniline) remained unchanged with the change of $[Ani]_T$ within the range of $[Ani]_T$ attained in the study. The linearity of the plots in Figure 1 would be necessary but not a sufficient condition to state that the fraction of free base as a function of $[Ani]_T$ remains constant. The aqueous pK_a values

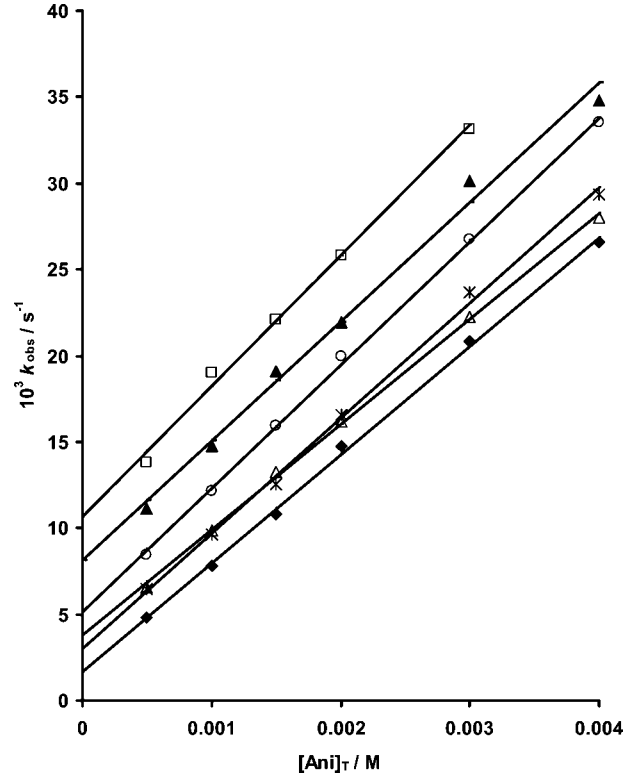

FIGURE 1. Plots showing the dependence of k_{obs} versus $[Ani]_T$ at different temperature: 30 (◆), 35 (Δ), 35 (*), 40 (○), 45 (▲), and 50 °C (□) in AcOH. The solid lines are drawn through the calculated data points using eq 1 and the kinetic parameters, k_s and k_n^{app} listed in Table 1.

(4) Blackburn, R. A. M.; Capon, B.; Mcritchie, A. C. *Biorg. Chem.* **1977**, *6*, 71.
(5) Grandos, A. M.; de Rossi, R. H. *J. Org. Chem.* **2001**, *66*, 1548.
(6) (a) Leng, S.-Y.; Ariffin, A.; Khan, M. N. *Int. J. Chem. Kinet.* **2004**, *36*, 316. (b) Sim, Y.-L.; Ariffin, A.; Khan, M. N. *Int. J. Chem. Kinet.* **2006**, *38*, 746.
(7) (a) Sim, Y.-L.; Ariffin, A.; Khan, M. N. *J. Org. Chem.* **2007**, *72*, 2392. (b) Cheong, M.-Y.; Ariffin, A.; Khan, M. N. *Indian J. Chem.* **2005**, *44A*, 2055. (c) Ahmad, W. H. W.; Ariffin, A.; Khan, M. N. *Indian J. Chem.* **2007**, *46A*, 416.

TABLE 1. Values of Rate Constants, k_s and k_n^{app}, Calculated from Equation *1* for the Cleavage of PAn in Pure and Mixed AcOH−CS Solvents Containing Ani[a]

AcOH (% v/v)	T (°C)	CS[b] (% v/v)	$10^4\ k_s$ (s^{-1})	$10\ k_n^{app}$ ($M^{-1}\ s^{-1}$)	N[c]	f_b[d]	$10\ k_n$[e] ($M^{-1}\ s^{-1}$)	$[Ani]_T$[f] range
100	30	0	16.5 ± 3.0[g]	63.0 ± 1.3[g]	6	0.146	432	5.0×10^{-4}−4.0×10^{-3}
100	30	0	13.8 ± 2.1	62.2 ± 0.9	6	0.132	471	5.0×10^{-4}−4.0×10^{-3}
100	35	0	38.2 ± 2.2	61.0 ± 0.9	6	0.158	386	5.0×10^{-4}−4.0×10^{-3}
100	35	0	29.9 ± 3.6	66.9 ± 1.5	6	0.163	410	5.0×10^{-4}−4.0×10^{-3}
100	40	0	54.2 ± 4.0	62.3 ± 1.8	6	0.18	346	5.0×10^{-4}−4.0×10^{-3}
100	40	0	51.5 ± 2.6	71.6 ± 1.1	6	0.18	398	5.0×10^{-4}−4.0×10^{-3}
100	45	0	81.4 ± 7.3	69.2 ± 3.0	6	0.199	348	5.0×10^{-4}−4.0×10^{-3}
100	50	0	107 ± 6	75.6 ± 3.0	6	0.231	327	5.0×10^{-4}−3.0×10^{-3}
99	35	1[h]	35.1 ± 3.6	58.4 ± 1.7	10	0.143	408	5.0×10^{-4}−4.0×10^{-3}
95	35	5[h]	32.5 ± 3.6	59.3 ± 0.5	10	0.161	368	5.0×10^{-4}−4.0×10^{-3}
90	35	10[h]	32.5 ± 1.1	59.5 ± 1.4	9	0.166	358	5.0×10^{-4}−4.0×10^{-3}
85	35	15[h]	31.7 ± 2.9	63.9 ± 1.1	10	0.198	323	5.0×10^{-4}−4.0×10^{-3}
80	35	20[h]	23.9 ± 2.4	61.7 ± 1.0	9	0.211	292	5.0×10^{-4}−4.0×10^{-3}
75	35	25[h]	20.4 ± 4.0	61.8 ± 1.9	10	0.22	281	5.0×10^{-4}−4.0×10^{-3}
70	35	30[h]	18.3 ± 2.8	60.7 ± 1.3	10	0.23	264	5.0×10^{-4}−4.0×10^{-3}
60	35	40[h]	6.94 ± 0.12	69.1 ± 0.7	9	0.295	234	5.0×10^{-4}−3.0×10^{-3}
50	35	50[h]	4.40 ± 2.80	75.6 ± 1.6	9	0.371	204	5.0×10^{-4}−3.0×10^{-3}
40	35	60[h]	9.70 ± 2.50	77.1 ± 1.6	8	0.465	166	5.0×10^{-4}−2.5×10^{-3}
30	35	70[h]	7.50 ± 1.60	80.5 ± 1.4	10	0.554	145	3.0×10^{-4}−2.0×10^{-3}
20	35	80[h]	12.4 ± 1.6	75.6 ± 1.7	7	0.729	104	3.0×10^{-4}−1.5×10^{-3}
10	35	90[h]	5.30 ± 1.00	54.7 ± 1.3	6	0.779	70.2	3.0×10^{-4}−1.3×10^{-3}
95	35	5[i]	30.9 ± 2.8	78.6 ± 1.3	10	0.204	385	5.0×10^{-4}−4.0×10^{-3}
90	35	10[i]	37.3 ± 5.6	86.8 ± 2.7	10	0.226	384	5.0×10^{-4}−4.0×10^{-3}
85	35	15[i]	30.9 ± 9.3	101 ± 5	10	0.277	365	5.0×10^{-4}−3.0×10^{-3}
80	35	20[i]	17.2 ± 2.5	121 ± 2	8	0.328	369	5.0×10^{-4}−3.0×10^{-3}
75	35	25[i]	13.2 ± 2.8	141 ± 2	8	0.404	349	5.0×10^{-4}−2.5×10^{-3}
70	35	30[i]	13.2 ± 2.9	151 ± 2	7	0.459	329	3.0×10^{-4}−2.0×10^{-3}
60	35	40[i]	8.1 ± 1.3	175 ± 1	7	0.613	285	3.0×10^{-4}−1.5×10^{-3}
50	35	50[i]	6.9 ± 2.0	171 ± 3	7	0.737	232	3.0×10^{-4}−1.3×10^{-3}
40	35	60[i]	−3.0 ± 1.8	158 ± 2	7	0.809	195	3.0×10^{-4}−1.3×10^{-3}
40	35	60[i]	0	154 ± 3	7	0.811	190	3.0×10^{-4}−1.3×10^{-3}
35	35	65[i]	3.8 ± 1.3	130 ± 2	6	0.849	153	3.0×10^{-4}−1.0×10^{-3}
30	35	70[i]	1.2 ± 32	110 ± 5	6	0.889	124	3.0×10^{-4}−1.0×10^{-3}
30	35	70[i]	2.7 ± 0.7	111 ± 1	6	0.837	133	3.0×10^{-4}−1.0×10^{-3}
25	35	75[i]	2.5 ± 0.7	89.3 ± 1.1	6	0.904	98.8	3.0×10^{-4}−1.0×10^{-3}
20	35	80[i]	4.3 ± 1.5	62.5 ± 14.8	6	0.786	79.5	3.0×10^{-4}−1.0×10^{-3}
20	35	80[i]	1.7 ± 0.8	67.6 ± 1.3	6	0.828	81.6	3.0×10^{-4}−1.0×10^{-3}
15	35	85[i]	1.2 ± 0.5	49.0 ± 0.7	6	0.836	58.6	3.0×10^{-4}−1.0×10^{-3}
10	35	90[i]	0.4 ± 0.6	32.0 ± 0.9	6	0.815	39.3	3.0×10^{-4}−1.0×10^{-3}
10	35	90[i]	1.0 ± 0.4	30.6 ± 0.7	6	0.794	38.5	3.0×10^{-4}−1.0×10^{-3}

[a] $[PAn_0] = 1.5 \times 10^{-4}$ M. [b] CS = cosolvent. [c] Total number of kinetic runs. [d] The values of f_b were calculated from eq 6 or eq 10 with $\delta_{Ani} = 1175$ $M^{-1}\ s^{-1}$ and δ_{ob} values listed in Table 2. [e] The values of k_n were calculated from eq 18 (i.e., $k_n = k_n^{app}/f_b$). [f] Total concentration range of aniline. [g] Error limits are standard deviations. [h] CS = CH_3CN. [i] CS = THF.

of benzoic acid, acetic acid, and anilinium ion are 4.20,[8] 4.76,[9] and 4.59,[8] respectively. The pK_a values of benzoic acid and acetic acid in dimethyl sulfoxide, DMSO (an aprotic organic solvent of ε about 48) are 11.0 and 12.3, respectively,[8] but the pK_a value of morpholinium ion in DMSO and aqueous solution are 8.7[8] and 8.36,[9] 8.82,[10] respectively. The ionization reactions of anilinium ion and acetic as well as benzoic acid are termed isoelectric and nonisoelectric ionization reactions, respectively. The increase in acetonitrile content from 2% to 70% v/v in mixed aqueous solvents increased the pK_a of benzylammonium and phenol from 9.16 to 9.26 and 10.17 to 13.38, respectively.[11] In view of these reports,[8−11] it is certain that the pK_a values of acetic acid and anilinium ion must be higher in a solvent of ε of ∼6 (glacial acetic acid) than that of ∼78.5 (water solvent). Significant reactivity of aniline with PAn in glacial acetic acid solution, where $[\text{acetic acid}]_T/[\text{aniline}]_T$ is in the range 3.4×10^4−4.3×10^3 M, indicates that the pK_a of anilinium ion is lower than that of acetic acid under such conditions.

Since the dielectric constant (ε) of glacial acetic acid solution is ∼6 and according to a very rough rule, solutions free of ion-pairing or other ionic aggregates at ionic concentrations in millimolar range require solvents with dielectric constants greater than 30,[8] it is not possible to determine the pK_a of anilinium ion and acetic acid in a solvent of ε of ∼6. However, the values of f_b under a variety of reaction conditions have been determined as follows. The values of absorbance (A_0) at the reaction time $t = 0$ were obtained at 275 nm from eq 2

$$A_{ob} = \delta_{app}[R0][1 - \exp(-k_{obs}t)] + A_0 \qquad (2)$$

where A_{ob} is the absorbance at 275 nm and any reaction time t and $[R_0]$, δ_{app}, k_{obs}, and A_0 represent the initial concentration of PAn, apparent molar extinction coefficient of the reaction mixture, pseudo-first-order rate constant and initial absorbance, respectively. Beer's law (i.e., eq 3) has been used to calculate the molar extinction coefficient (δ_{ob}) of aniline at 275 nm in 96% v/v water solvent containing 4% v/v CH_3CN and 0.1 M in both NaOH and HCl. The values of δ_{ob} turned out to be ∼0 and 1175 ± 42 $M^{-1}\ cm^{-1}$ at 0.1 M HCl and 0.1 M NaOH,

(8) Rithchie, C. D. *Physical Organic Chemistry*, 2nd ed.; Marcel Decker, Inc.: New York, Basel, 1990.
(9) Cordes, E. H.; Jenks, W. P. *J. Am. Chem. Soc.* **1962**, *84*, 4319.
(10) Knier, B. L.; Jencks, W. P. *J. Am. Chem. Soc.* **1980**, *102*, 6789.
(11) Khan, M. N.; Ariffin, Z.; George, A.; Wahab, I. A. *Int. J. Chem. Kinet.* **2000**, *32*, 146.

TABLE 2. Values of α and δ_{ob}, Calculated from Equation *3* Using A_0

AcOH (% v/v)	CS[a] (% v/v)	10^4 PAn[b] (M)	10^2 α	δ_{ob} M^{-1} cm^{-1}	*N*[c]	*T* (°C)	$[Ani]_T$[d] range (M)
0	96[e]	0	0	1175 ± 42[f]	4	35	5.0×10^{-4}−2.0×10^{-3}
0	96[e]	0	0	1176 ± 51	3	35	5.0×10^{-4}−1.5×10^{-3}
0	96[g]	0	1.04 ± 0.14[f]	0.8 ± 0.6	6	35	5.0×10^{-4}−4.0×10^{-3}
0	100[h]	0	4.1 ± 0.4	955 ± 3	9	35	3.0×10^{-4}−2.0×10^{-3}
0	100[i]	0	0.9 ± 0.4	1008 ± 3	8	35	3.0×10^{-4}−1.8×10^{-3}
0	100[j]	0	0	1022 ± 10	8	35	3.0×10^{-4}−1.8×10^{-3}
100	0	0	4.9 ± 0.2	197 ± 1	6	30	5.0×10^{-4}−4.0×10^{-3}
100	0	0	3.0 ± 0.4	214 ± 2	6	35	5.0×10^{-4}−4.0×10^{-3}
100	0	0	3.3 ± 0.2	236 ± 1	6	40	5.0×10^{-4}−4.0×10^{-3}
100	0	0	3.7 ± 0.4	258 ± 2	6	45	5.0×10^{-4}−4.0×10^{-3}
100	0	0	3.3 ± 0.5	285 ± 2	6	50	5.0×10^{-4}−4.0×10^{-3}
100	0	1.5	34.3 ± 0.4	171 ± 2	6	30	5.0×10^{-4}−4.0×10^{-3}
100	0	1.5	34.3 ± 1.5	155 ± 6	6	30	5.0×10^{-4}−4.0×10^{-3}
100	0	1.5	41.1 ± 1.3	186 ± 6	6	35	5.0×10^{-4}−4.0×10^{-3}
100	0	1.5	32.1 ± 0.6	191 ± 2	6	35	5.0×10^{-4}−4.0×10^{-3}
100	0	1.5	37.1 ± 0.9	212 ± 4	6	40	5.0×10^{-4}−4.0×10^{-3}
100	0	1.5	31.5 ± 1.4	211 ± 6	6	40	5.0×10^{-4}−4.0×10^{-3}
100	0	1.5	29.9 ± 1.1	234 ± 5	6	45	5.0×10^{-4}−4.0×10^{-3}
100	0	1.5	26.7 ± 2.4	272 ± 12	5	50	5.0×10^{-4}−3.0×10^{-3}
99	1[j]	1.5	20.8 ± 0.4	168 ± 2	10	35	5.0×10^{-4}−4.0×10^{-3}
95	5[j]	1.5	20.5 ± 0.3	189 ± 1	10	35	5.0×10^{-4}−4.0×10^{-3}
90	10[j]	1.5	20.8 ± 2.6	195 ± 12	10	35	5.0×10^{-4}−4.0×10^{-3}
85	15[j]	1.5	17.9 ± 0.7	233 ± 4	10	35	5.0×10^{-4}−4.0×10^{-3}
80	20[j]	1.5	17.7 ± 2.8	248 ± 13	10	35	5.0×10^{-4}−4.0×10^{-3}
75	25[j]	1.5	18.1 ± 0.7	258 ± 3	10	35	5.0×10^{-4}−4.0×10^{-3}
70	30[j]	1.5	17.2 ± 2.9	270 ± 1	10	35	5.0×10^{-4}−4.0×10^{-3}
60	40[j]	1.5	10.3 ± 2.2	347 ± 13	9	35	5.0×10^{-4}−3.0×10^{-3}
50	50[j]	1.5	8.2 ± 2.1	436 ± 12	9	35	5.0×10^{-4}−3.0×10^{-3}
40	60[j]	1.5	9.4 ± 2.0	546 ± 13	8	35	5.0×10^{-4}−2.5×10^{-3}
30	70[j]	1.5	12.6 ± 1.5	651 ± 13	10	35	3.0×10^{-4}−2.0×10^{-3}
20	80[j]	1.5	13.4 ± 0.8	857 ± 8	7	35	3.0×10^{-4}−1.5×10^{-3}
10	90[j]	1.5	24.5 ± 1.3	915 ± 17	6	35	3.0×10^{-4}−1.3×10^{-3}
95	5[k]	1.5	20.5 ± 0.5	240 ± 3	10	35	5.0×10^{-4}−4.0×10^{-3}
90	10[k]	1.5	22.6 ± 1.4	66 ± 7	10	35	5.0×10^{-4}−4.0×10^{-3}
85	15[k]	1.5	21.3 ± 1.8	325 ± 10	9	35	5.0×10^{-4}−3.0×10^{-3}
80	20[k]	1.5	20.8 ± 0.5	385 ± 3	8	35	5.0×10^{-4}−3.0×10^{-3}
75	25[k]	1.5	19.5 ± 1.1	475 ± 7	8	35	5.0×10^{-4}−2.5×10^{-3}
70	30[k]	1.5	21.0 ± 0.3	539 ± 2	7	35	5.0×10^{-4}−2.0×10^{-3}
60	40[k]	1.5	21.0 ± 0.5	720 ± 6	7	35	5.0×10^{-4}−1.5×10^{-3}
50	50[k]	1.5	21.2 ± 0.4	866 ± 5	7	35	3.0×10^{-4}−1.3×10^{-3}
40	60[k]	1.5	22.5 ± 0.6	950 ± 8	7	35	3.0×10^{-4}−1.0×10^{-3}
40	60[k]	1.5	21.6 ± 0.6	953 ± 7	6	35	3.0×10^{-4}−1.3×10^{-3}
35	65[k]	1.5	21.0 ± 0.7	998 ± 10	6	35	3.0×10^{-4}−1.0×10^{-3}
30	70[k]	1.5	19.2 ± 1.9	1045 ± 28	5	35	3.0×10^{-4}−1.0×10^{-3}
30	70[k]	1.5	23.7 ± 0.8	984 ± 13	6	35	3.0×10^{-4}−1.0×10^{-3}
25	75[k]	1.5	26.1 ± 1.4	1062 ± 22	6	35	3.0×10^{-4}−1.0×10^{-3}
20	80[k]	1.5	27.5 ± 3.1	923 ± 48	6	35	3.0×10^{-4}−1.0×10^{-3}
20	80[k]	1.5	28.3 ± 0.6	973 ± 10	6	35	3.0×10^{-4}−1.0×10^{-3}
15	85[k]	1.5	28.1 ± 2.8	982 ± 43	6	35	3.0×10^{-4}−1.0×10^{-3}
10	90[k]	1.5	24.2 ± 2.7	958 ± 42	6	35	3.0×10^{-4}−1.0×10^{-3}
10	90[k]	1.5	28.1 ± 1.7	933 ± 27	6	35	3.0×10^{-4}−1.0×10^{-3}

[a] CS = cosolvent. [b] PAn = phthalic anhydride. [c] Total number of kinetic runs. [d] Total concentration range of aniline. [e] Water cosolvent contains 4% v/v CH_3CN and 0.1 M NaOH. [f] Error limits are standard deviations. [g] Water cosolvent contains 4% v/v CH_3CN and 0.1 M HCl. [h] Pure THF solvent. [i] Pure CH_3CN solvent. [j] CS = CH_3CN cosolvent. [k] CS = THF.

SCHEME 2

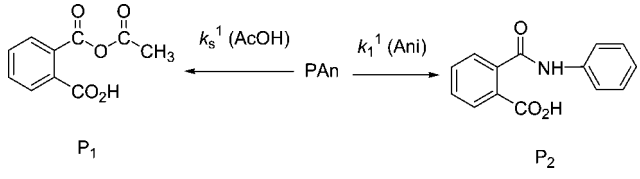

respectively. These results show that the values of molar extinction coefficient of free aniline base (δ_{Ani}) and protonated aniline (δ_{AniH+}) at 275 nm are 1175 and ∼0 M^{-1} cm^{-1}, respectively. The values of A_0, obtained at 275 nm and within $[Ani]_T$ in the range 3.0×10^{-4}−1.8×10^{-3} M in 100% CH_3CN solvent fit to eq 3 with percent residual error (RE = 100 × $[(A_{0i} - A_{calci})/A_{0i}]$ where A_{0i} and A_{calci} represent, respectively, the observed and calculated absorbance at *i*th $[Ani]_T$) of ≤0.7%. Similar observations were also obtained in 100% THF solvent. In eq 3, α represents absorbance due to solvent and other additives (if present). The least-squares calculated values of α and δ_{ob} at 275nm and 100% CH_3CN and THF are summarized in Table 2.

$$A_0 = \alpha + \delta_{ob}[Ani]_T \quad (3)$$

It is known from the literature that the absorption spectra may or may not change in different solvents. In order to find out the effects of mixed H_2O−CH_3CN and H_2O−THF solvents on the absorption spectra of aniline (Ani), a series of UV absorption spectra was obtained at 35 °C for the mixed aqueous

solutions containing 1.0×10^{-3} M Ani and CH_3CN content ranging from 1% to 60% v/v at 0.1 M NaOH and 1% to 90% v/v at 0.1 M HCl. Similar observations were obtained in H_2O-THF solvents. The values of A_{ob} at 275 nm as a function of the content of CH_3CN and THF are summarized in Table 1 in Supporting Information. It is evident from these results that there is ~8.4% decrease in A_{ob} with the increase in CH_3CN content from 1% to 60% at 0.1 M NaOH. Similarly, A_{ob} values decrease by ~4.6% with the increase in THF content from 30% to 50% v/v, while the change in THF content from 1% to 30% v/v has no effect on A_{ob} at 0.1 M NaOH. The values of A_{ob} remained almost unchanged at nearly zero with change in the contents of both CH_3CN and THF from 1% to 90% v/v at 0.1 M HCl (CH_3CN) and 1.0 M HCl (THF).

By definition, $f_b = [Ani]/[Ani]_T$ with $[Ani]_T = [Ani] + [AniH^+]$. The absorbance ($A_{ob}$) of aqueous solution containing Ani and $AniH^+$ only (where absorbance due to solvent is zero) may be expressed as

$$A_{ob} = \delta_{Ani}[Ani] + \delta_{AnH}[AniH^+] = \{f_b\delta_{Ani} + (1 - f_b)\delta_{AniH^+}\}[Ani]_T \quad (4)$$

Equation 4 can be rearranged to give eq 5

$$f_b = (\delta_{ob} - \delta_{AniH^+})/(\delta_{Ani} - \delta_{AniH^+}) \quad (5)$$

where $\delta_{ob} = A_{ob}/[Ani]_T$. Since $\delta_{AniH+} \approx 0$ at 275 nm in both pure and mixed H_2O-CH_3CN and H_2O-THF solvents, eq 5 is reduced to eq 6:

$$f_b = \delta_{ob}/\delta_{Ani} \quad (6)$$

The values of δ_{Ani}, obtained in 96% v/v water, for pure water ($\varepsilon = 78$) and pure acetonitrile ($\varepsilon = 37$) as well as THF ($\varepsilon = 8$) (Table 2), differ from each other by <19%. The values of δ_{Ani} at 275 nm of 1010 and 955 M^{-1} cm^{-1} for pure CH_3CN and THF, respectively, differ by <6%. Almost all δ_{ob} values in Table 2 were obtained in pure AcOH and mixed $AcOH-CH_3CN$ and $AcOH-THF$ solvents. However, since the values of δ_{Ani} decreases by less than 19% with change of solvent from 96% v/v H_2O to 100% CH_3CN or 100% THF, the values of f_b were approximately determined from eq 6 considering the δ_{Ani} value (= 1175 M^{-1} cm^{-1}) obtained at 0.1 M NaOH in mixed H_2O-CH_3CN solvent containing 96% v/v H_2O.

The values of A_0, obtained at 275 nm, 30 °C, and within $[Ani]_T$ range $5.0 \times 10^{-4}-4.0 \times 10^{-3}$ M, fit to eq 3, and the least-squares calculated values of α and δ_{ob} at different temperatures are shown in Table 2. These results show that α values are almost independent of temperature, but δ_{ob} values increase slightly with the increase of temperature, which could be attributed to a modest increase in f_b with increasing temperature. The values of A_0 and A_∞ calculated from eq 2 where $A_\infty = A_0 + \delta_{app}[R_0]$ (with $[R_0]$ representing the initial concentration of PAn), at a constant temperature and different $[Ani]_T$ were also found to fit to eq 3 with A_0 or A_∞. The least-squares calculated values of α and δ_{ob} at different temperature for A_0 and A_∞ are shown in Table 2 and Table 2 in Supporting Information, respectively. The reliable fit of the data to eq 3 is evident from the standard deviations associated with the calculated parameters, α and δ_{ob}, and from the few typical plots of Figure 2 where the solid lines are drawn through the calculated data points. The values of α corresponding A_0 reveal significant absorption due to PAn at 275 nm. The values of δ_{ob} for A_∞ are larger than the corresponding δ_{ob} values for A_0 by values ranging within 25−73 M^{-1} cm^{-1} at 30−50 °C (Table 2 and Table 2, Supporting Information). Although these differences in δ_{ob} values are small, they exist beyond the limits of experimental uncertainty and these observations may be explained in the following text.

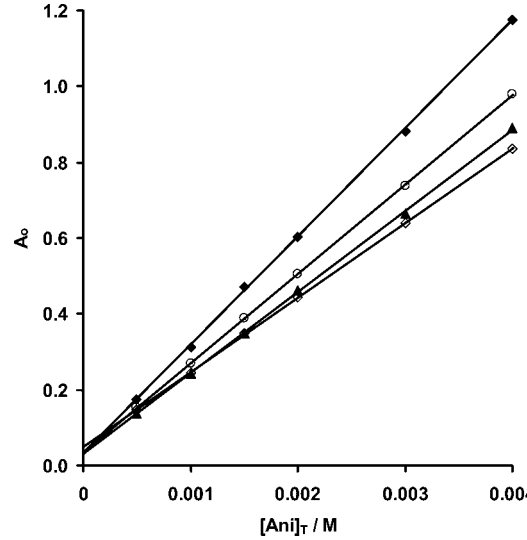

FIGURE 2. Plots showing the dependence of A_0 versus $[Ani]_T$ at different temperatures: 30 (◇), 35 (▲), 40 (○), and 50 °C (◆) in AcOH and absence of phthalic anhydride. The solid lines are drawn through the calculated data points using eq 3 and the parameters α and δ_{ob}, listed in Table 2.

It is apparent from Scheme 2 and eq 2 that

$$A_0 = \delta_{sol}[Sol] + \delta_{Ani}[Ani] + \delta_{AniH^+}[AniH^+] + \delta_{PAn}[PAn_0] \quad (7)$$

where δ represents molar extinction coefficient, Sol is solvent, and $[PAn_0]$ is the concentration of PAn at reaction time, $t = 0$. The fact that $\delta_{AniH^+} \approx 0$ and $f_b = [Ani]/[Ani]_T$ (where $[Ani]_T = [Ani] + [AniH^+]$) reduces eq 7 to eq 8:

$$A_0 = \delta_{sol}[Sol] + \delta_{Ani}f_b[Ani]_T + \delta_{PAn}[PAn_0] \quad (8)$$

which is similar to eq 3 with

$$\alpha^0 = \delta_{sol}[Sol] + \delta_{PAn}[PAn_0] \quad (9)$$

and

$$\delta_{ob} = \delta_{Ani}f_b \quad (10)$$

In view of eq 2 and Scheme 2,

$$A_\infty = \delta_{sol}[Sol] + \delta_{P1}[P1] + \delta_{P2}[P2] + \delta_{Ani}[Ani'] \quad (11)$$

where [Ani′] represents the concentration of unreacted free aniline base. The concentration of reacted free aniline base, [Ani″], is equal to $[P_2]$ (i.e., $[Ani''] = [P_2]$). If $F_1 = k_s/(k_s + k_n^{app}[Ani]_T)$ and $F_2 = k_n^{app}[Ani]_T/(k_s + k_n^{app}[Ani]_T)$ then $F_1 + F_2 = 1$ with $F_1 = [P_1]/[PAn_0]$ and $F_2 = [P_2]/[PAn_0]$ and application of these relationships to eq 11 gives eq 12:

$$A_\infty = \delta_{sol}[Sol] + \delta_{P1}F_1[PAn_0] + \delta_{P2}F_2[PAn_0] + \delta_{Ani}[Ani'] \quad (12)$$

In a typical kinetic run, the reaction mixture containing 100% v/v AcOH and 1.5×10^{-4} M PAn was allowed to progress at 30 °C for the reaction period of >7 half-lives (based upon k_s value, Table 1). The absorbance, A_{ob}, at 275 nm remained almost unchanged within the reaction period of >7 half-lives which

reveals that $\delta_{P1} \approx \delta_{PAn}$ at 275 nm. The values of δ_{P2} and δ_{PAn} are 7.77×10^3 and 2.24×10^3 M^{-1} cm^{-1} at 275 nm, respectively.

The values of F_1 and F_2 decrease and increase, respectively, with the increase in $[Ani]_T$ at the constant concentration and composition of mixed solvent components. The values of F_2 were found to follow the linear relationship: $F_2 = c + m[Ani]_T$ within $[Ani]_T$ range 1.0×10^{-3}−4.0×10^{-3} M at a constant temperature within its range 30−45 °C and within 1.0×10^{-3}−3.0×10^{-3} M at 50 °C. The respective calculated values of intercept (c) and slope (m) are 0.79 ± 0.02 and 43.3 ± 8.0 M^{-1} at 30 °C, 0.62 ± 0.04 and 71.9 ± 14.2 M^{-1} at 35 °C, 0.40 ± 0.04 and 99.7 ± 14.9 M^{-1} at 45 °C, and 0.34 ± 0.04 and 106 ± 15 M^{-1} at 50 °C. Although a perfect linearity is impossible to achieve, maximum residual error (MRE = $100 \times (F_2 - F_{2cald})/F_2$ where F_{2cald} values were calculated from the relationship $F_{2calcd} = c + m[Ani]_T$ with least-squares calculated parameters c and m) turned out to be −2.6%, −5.9%, −8.4%, and −9.3% at respective temperatures 30, 35, 45, and 50 °C and the lowest $[Ani]_T$ (= 1.0×10^{-3} M). The combination of the relationships $F_2 = c + m[Ani]_T$, $F_1 + F_2 = 1$, and eq 12 gives eq 13:

$$A_\infty = \delta_{sol}[Sol] + \{\delta_{P1} + c(\delta_{P2} - \delta_{P1})\}[PAn_0] + \{m(\delta_{P2} - \delta_{P1})[PAn_0] + \delta_{Ani} f_b'\}[Ani]_T \quad (13)$$

where $f_b' = [Ani']/[Ani]_T$. Equation 13 is similar to eq 3 with

$$\alpha^\infty = \delta_{sol}[Sol] + \{\delta_{P1} + c(\delta_{P2} - \delta_{P1})\}[PAn_0] \quad (14)$$

and

$$\delta_{ob}{}^\infty = m(\delta_{P2} - \delta_{P1})[PAn_0] + \delta_{Ani} f_b' \quad (15)$$

where superscript "∞" merely indicates that these values are obtained from eq 3 with A_0 replaced by A_∞. It may be noted that the observed data point at $[Ani]_T = 5.0 \times 10^{-4}$ M showed negative deviation from linearity of the plot of A_∞ versus $[Ani]_T$ by 16%, 17%, 17%, and 19% at 30, 35, 45 and 50 °C, respectively. Such significant negative deviations are due to relatively large negative deviations of observed data points from linearity due to $F_2 = c + m[Ani]_T$ under such conditions. Equations 10 and 15 predict larger value of $\delta_{ob}{}^\infty$ than that of δ_{ob} for the same set of kinetic runs because $\delta_{P2}/\delta_{P1} \geq 3.5$ and $m \geq 43$ M^{-1} at ≥30 °C.

Effects of [Aniline] on the Cleavage of PAn in Mixed AcOH−CH_3CN Solvents at 35 °C. In order to discover the effects of varying concentration of [Ani] and AcOH on the rate constants for the reactions of PAn with AcOH and aniline, a few kinetic runs were carried at a constant composition of mixed AcOH−CH_3CN solvent and within total aniline concentration ($[Ani]_T$) range $\geq 2.5 \times 10^{-4}$ to $\leq 4.0 \times 10^{-3}$ M. The rate constants, k_{obs}, were found to fit to eq 1 and the least-squares calculated values of k_s and k_n^{app} at different contents of AcOH are summarized in Table 1. The reliable fit of observed data to eq 1 is evident from the standard deviations associated with the calculated kinetic parameters, k_s and k_n^{app}, and from some typical plots of Figure 3 where solid lines are drawn through the calculated data points.

The values of A_0, calculated from eq 2, showed satisfactory fit to eq 3. The least-squares calculated values of α and δ_{ob} at different contents of CH_3CN ranging from 1−90% v/v are summarized in Table 2. The extent of reliable fit of the data (A_0 versus $[Ani]_T$) to eq 3 is evident from the standard deviations associated with calculated parameters, α and δ_{ob} (Table 2), and

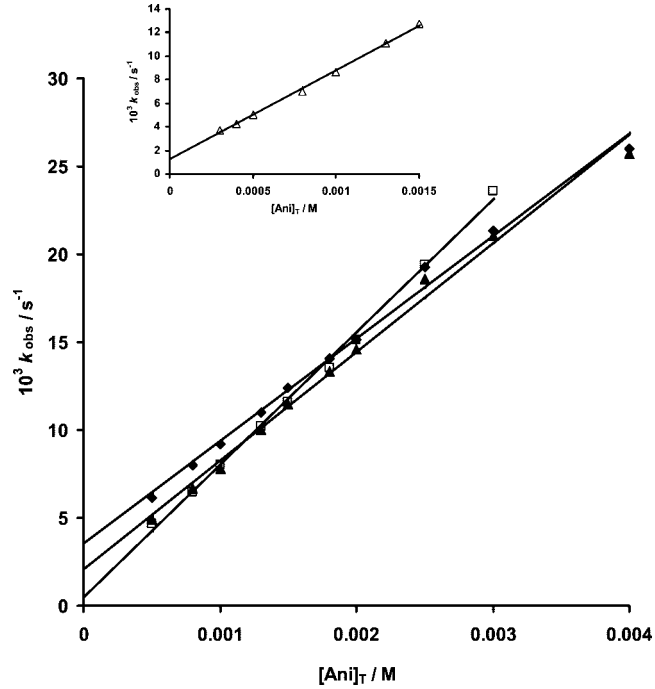

FIGURE 3. Plots showing the dependence of k_{obs} versus $[Ani]_T$ at 1% (◆), 25% (▲), 50% (*), and 80% (Δ) v/v CH_3CN in mixed CH_3CN−AcOH solvents. The solid lines are drawn through the calculated data points using eq 1 and the kinetic parameters, k_s and k_n^{app}, listed in Table 1.

from a few typical plots of A_0 versus $[Ani]_T$ of Figure II (Supporting Information) where solid lines are drawn through the least-squares calculated data points. The calculated values of δ_{ob} were used to calculate f_b from eq 10 with $\delta_{Ani} = 1175$ M^{-1} cm^{-1}, and these values of f_b are shown in Table 2. The calculated values of A_∞ ($A_\infty = A_0 + \delta_{app}[R_0]$, eq 2) were also treated with eq 3 where A_0, α, and δ_{ob} were replaced by A_∞, α^∞, and $\delta_{ob}{}^\infty$, respectively, and the least-squares calculated values of α^∞ and $\delta_{ob}{}^\infty$ are summarized in Table 2 (Supporting Information).

Effects of [Aniline] on the Cleavage of PAn in mixed AcOH−THF Solvents at 35 °C. Despite the fact that both THF and CH_3CN are aprotic solvents and useful for organic synthesis, their various physicochemical properties are significantly different from each other. Furthermore, the value of ε of THF is similar to that of AcOH, and hence change in the composition of mixed solvent components, THF and AcOH, is not expected to change the ε values of mixed AcOH−THF solvents. Thus, the mixed AcOH−THF system is particularly useful for reaction rate study where one of the rate-affecting solvent parameters (i.e., ε) could be kept nearly constant with the change in the composition of mixed solvents. A series of kinetic runs was carried out for the cleavage of PAn at different values of $[Ani]_T$ ranging from $\geq 3.0 \times 10^{-4}$ to $\leq 4.0 \times 10^{-3}$ M at a constant content of THF in mixed AcOH solvent. The values of k_{obs} fit to eq 1 and the least-squares calculated values of k_s and k_n^{app} at different contents of THF are summarized in Table 1. The data fit to eq 1 is satisfactory as evident from the standard deviations associated with the calculated parameters and from a few typical plots of Figure 4 where the observed data points are not significantly different from the corresponding predicted data points based upon eq 1.

The values of f_b at different contents of THF were obtained from the Beer's plot of A_0, calculated from eq 2, versus $[Ani]_T$.

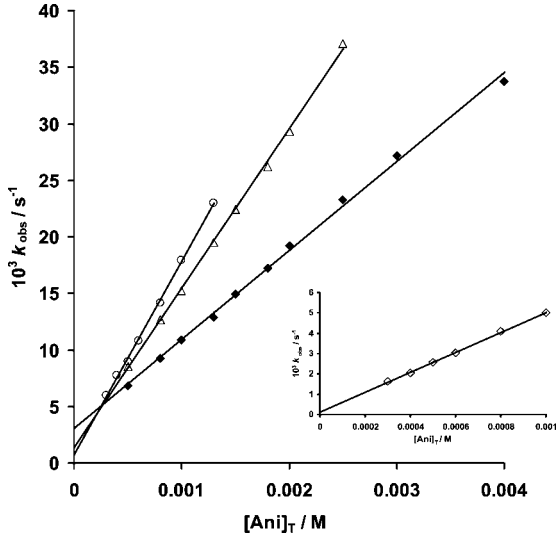

FIGURE 4. Plots showing the dependence of k_{obs} versus $[Ani]_T$ at 5% (◆), 25% (Δ), 50% (○), and 85% (◇) v/v THF in mixed THF−AcOH solvents. The solid lines are drawn through the calculated data points using eq 1 and the kinetic parameters, k_s, and least-squares calculated values of k_s and k_n^{app} listed in Table 1.

The values of A_0 at a constant content of THF and different values of $[Ani]_T$ fit to eq 3. The least-squares calculated values of α and δ_{ob} at different contents of THF ranging from 5−90% v/v are shown in Table 2. The standard deviations, associated with the calculated parameters (α and δ_{ob}), and a few typical plots of A_0 versus $[Ani]_T$ of Figure II (Supporting Information), where solid lines are drawn through the calculated data points, reveal the extent of reliability of the fit of the data to eq 3. The calculated values of δ_{ob} were used to calculate f_b from eq 10 with $\delta_{Ani} = 1175\ M^{-1}\ cm^{-1}$. These values of f_b are summarized in Table 2. The calculated values A_∞ ($A_\infty = A_0 + \delta_{app}[R_0]$, eq 2) were also attempted to fit to eq 3 with replacement of A_0, α, and δ_{ob} by respective A_∞, α^∞ and δ_{ob}^∞, and the least-squares calculated values of α^∞ and δ_{ob}^∞ are shown in Table 2 (Supporting Information).

Discussion

Effects of Mixed AcOH−CH_3CN and AcOH−THF on the Fraction of Free Aniline Base (f_b). In order to discuss the effects of aprotic organic cosolvent, such as acetonitrile and tetrahydrofuran (THF), the absorbance (A_{ob}) of mixed solvent AcOH−CH_3CN containing 8.0×10^{-4} M aniline (stock solution of aniline was prepared in pure CH_3CN) was measured at 275 nm. The values of A_{ob} at different % v/v content of CH_3CN are shown graphically in Figure 5. Similar observations were obtained in mixed AcOH−THF (the stock solution of aniline was prepared in THF) and these results are also shown graphically in Figure 5.

The value of A_{ob} is related to f_b through the relationship $A_{ob} = A_{sol} + f_b\delta_{Ani}[Ani]_T$ where A_{sol} represents absorbance due to solvent. As discussed earlier, the values of δ_{Ani} are approximately independent of % v/v content (X) of CH_3CN and THF in mixed aqueous solvents (Table 2 and Table 2, Supporting Information). Thus, at a constant $[Ani]_T$ ($= 8.0 \times 10^{-4}$ M), A_{ob} is expected to be directly proportional to f_b because $A_{sol} \approx 0$ at 275 nm. In view of the facts mentioned earlier in the text, the increase in the content of aprotic organic cosolvent (such as CH_3CN and THF), in mixed AcOH−CH_3CN and AcOH−THF solvents containing a constant concentration of aniline is expected to increase the pK_a of AcOH more strongly compared to that of anilinium ion. This characteristic effect of mixed acetic acid-aprotic organic cosolvent predicts that the increase in the content of organic solvent CH_3CN and THF in mixed acetic acid solvent should increase the values of f_b. It is evident from Figure 5 that the values of A_{ob} ($\propto f_b$) increase almost linearly with the increase in the content of THF from 10 to 60% v/v followed by an independent region within ∼70% to 100% v/v THF, but the values of A_{ob} remained almost independent of the content of CH_3CN within its range 10−20% v/v followed by a nonlinear increase within ∼40−100% v/v CH_3CN. The shape of the plot of Figure 5 for CH_3CN is not exactly similar to that for THF, which could be attributed to some characteristic different structural and solution properties of CH_3CN and THF.

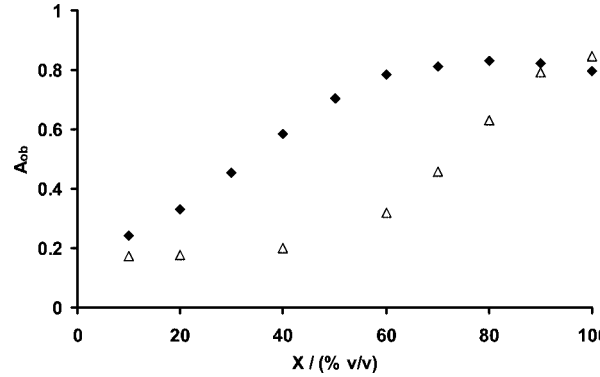

FIGURE 5. Plots showing the dependence of A_{ob} (at 275 nm) versus percent content of organic cosolvent, X (v/v) for X = CH_3CN (Δ) and X = THF (◆) in mixed X−AcOH solvents containing 8.0×10^{-4} M aniline.

TABLE 3. Dipole Moment (μ), Dielectric Constant (ε), Cohesive Energy Density (D_{ce}), and Hdrogen Bonding Energy (E^{HB}) of Water and Some Organic Solvents (25°C)[a]

solvent	μ (debye)	ε	D_{ce} (cal cm^{-3})	E^{HB} (kcal mol^{-1})
H_2O	1.855	78.5	550.2	
AcOH		6.13[b]		
HCOOH	1.82	58.5		
CH_3CN	3.44	37[b]	139.2	2.3
THF		7.6[c]	86.9	
dioxane	0.45	2.21	94.7	0

[a] Reference 13. [b] Reference 14. [c] Reference 8.

Alkanols have been shown to exist in monomeric, dimeric, trimeric,..., and *n*-meric forms due to intermolecular hydrogen bonding.[12] Acetic acid, containing both carbonyl oxygen (hydrogen bond acceptor site) and hydroxyl oxygen (both hydrogen bond donor and acceptor site), may also be expected to exist in monomeric AcOH, dimeric $(AcOH)_2$, trimeric $(AcOH)_3$,.., and *n*-meric $(AcOH)_n$ forms through both intra- and intermolecular hydrogen-bonded network. The monomeric acetic acid, AcOH, is apparently most reactive toward free aniline base, Ani. Although both acetonitrile and THF are aprotic organic solvent, they differ significantly in various physicochemical properties (Table 3). The aqueous mixtures of acetonitrile and THF have been characterized as typically nonaqueous (TNA)

(12) (a) Grunwald, E.; Pan, K.-C.; Effio, A. *J. Phys. Chem.* **1976**, *80*, 2937. (b) Khan, M. N. *Int. J. Chem. Kinet.* **1987**, *19*, 757. (c) Khan, M. N.; Ariffin, Z. *Langmuir* **1996**, *12*, 261. (d) Khan, M. N.; Ariffin, Z. *Langmuir* **1997**, *13*, 6626. (e) Khan, M. N. *J. Phys. Chem.* **1998**, *92*, 6273. (f) Khan, M. N.; Audu, A. A. *Int. J. Chem. Kinet.* **1990**, *22*, 37.

and typically aqueous (TA) solutions, respectively.[13] The increase in the content of CH_3CN or THF in mixed glacial acetic acid solvent (i) decreases the total concentration of glacial acetic acid, $[AcOH]_T$, which in turn decreases [AcOH] (concentration of monomeric AcOH) and (ii) increases the difference of pK_a (ΔpK_a) of acetic acid and anilinium ion. Both the decrease in [AcOH] and increase in ΔpK_a should increase f_b and consequently it should increase A_{ob}.

The values of A_{ob} are independent of the content of CH_3CN within its range 10−20% v/v, while such observations are not detectable in the presence of THF (Figure 5). These observations may qualitatively be explained as follows. It is well-known that TNA organic cosolvent, such as acetonitrile, diminishes the degree of long-range order in highly aqueous TNA solvents relative to water and as a consequence, acetonitrile is a water-structure-breaking cosolvent. Similarly, TA organic cosolvent, such as THF, is known as a water-structure-forming cosolvent in water-rich region.[13] If we assume that such solution properties of CH_3CN and THF remain unchanged with the change from water to glacial acetic acid, then the acetic acid-structure-breaking ability of CH_3CN is expected to increase [AcOH] in the acetic acid-rich region (i.e., ca. ≤ 20% v/v CH_3CN) which is expected to decrease f_b. It is now apparent that the increase in the content of CH_3CN in mixed acetic acid solvent causes two opposite effects on f_b: (i) an increase in f_b due to decrease in $[AcOH]_T$ as well as increase in ΔpK_a and (ii) a decrease in f_b due to acetic acid-structure-breaking ability of CH_3CN. It seems that these two opposite effects of CH_3CN increasing content counterbalance to each other and as a consequence f_b value remain unchanged at ≤20% v/v CH_3CN. However, the factors that increase f_b become increasingly dominant at ≥40% v/v CH_3CN. The plot for THF in Figure 5 reveals that the effect of acetic acid-structure-forming ability of THF on f_b remains insignificant compared to the effects on f_b of (i) increase in ΔpK_a and (ii) decrease in $[AcOH]_T$ due to increase in the content of THF in mixed acetic acid solvents. These effects have caused $f_b \approx 1$ at ≥70% v/v THF.

Mechanistic Explanations of Acetolysis and Anilinolysis of PAn in Mixed AcOH−CH_3CN and AcOH−THF Solvents. The maximum contributions of k_s compared to $k_n^{app}[Ani]_T$, obtained at the lowest values of $[Ani]_T$, are <25% at ≥10% v/v AcOH and <50% at <95% v/v AcOH for mixed AcOH−CH_3CN solvent system (Table 1). Because of the considerably low contribution of k_s compared to $k_n^{app}[Ani]_T$ in eq 1, the calculated values of k_s may be considered as less reliable.[15] However, although the values of k_s are not very reliable, k_s values seem to be independent of $[AcOH]_T$ within AcOH content range 10−60% v/v followed by an almost linear increase with $[AcOH]_T$ within ≥60−99% v/v AcOH (Figure 6a). Similar observations were obtained in the reaction of H_2O with ionized phenyl salicylate in mixed H_2O−CH_3CN solvent.[12b] A quantitative interpretation of pseudo-first-order rate constants for solvolytic reactions in mixed aqueous−organic cosolvent or mixed organic solvent-organic cosolvent is extremely difficult due to lack of general theoretical model or models caused by our lack of understanding about highly dynamic and complex structural network at the molecular level of these solvent systems. As a consequence, qualitative and empirical approaches are often used to rationalize such kinetic data.[1]

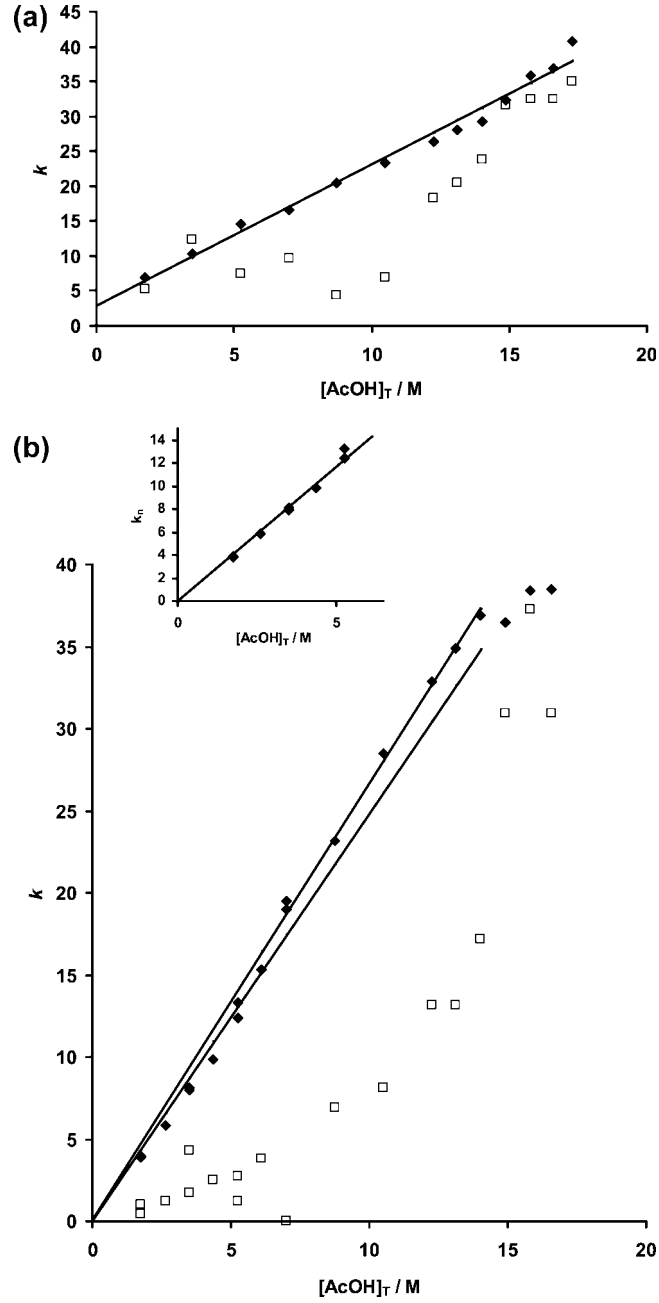

FIGURE 6. (a) The plots showing the dependence of k versus $[AcOH]_T$ for $k = k_n$ M^{-1} s^{-1}(◆) and $k = 10^4$ k_s s^{-1}(*) in mixed CH_3CN−AcOH solvents. (b) The plots showing the dependence of k versus $[AcOH]_T$ for $k = k_n$ M^{-1} s^{-1} (◆) and $k = 10^4$ k_s s^{-1} (*) in mixed THF−AcOH solvents.

A qualitative explanation for the nonlinear variation of k_s with the percent content of AcOH in mixed acetonitrile solvent may be described in terms of the concept of polarization of monomeric AcOH molecules such as **2** where B is the basic site of either RB = CH_3CN or THF. The nucleophilicity of the polarized AcOH molecule (**2**) is expected to be sufficiently increased compared to that of nonpolarized AcOH. Thus, as the percent content of RB increase, the content or concentration of **2** also increases, which causes an increase in the rate of acetolysis. At the same time, the total concentration of acetic acid $[AcOH]_T$, decreases, which in turn decreases the rate of

(13) Engberts, J. B. F. N. In *Water, a Comprehensive Treatise*; Franks, F., Ed.; Plenum: New York, 1979; Vol. 6, Chapter 4.
(14) Anantakrishnan, S. V. *J. Sci. Indust. Res.* **1971**, *30*, 319.
(15) Khan, M. N. Micellar Catalysis. In *Surfactant Science Series*; CRC Press, Taylor & Francis Group: Boca Raton, FL. 2006; Vol. 133, p 418.

acetolysis. These two opposing effects probably counterbalance each other in the RB-rich region, i.e., within CH_3CN content range of ~40−90% v/v, in the acetolysis of PAn and thus leads to an almost $[AcOH]_T$-independent rate of acetolysis (Figure 6a). Nearly linear increase in k_s with the increase in the content of AcOH at >60% v/v AcOH is merely due to increasing effect of $[AcOH]_T$ on [AcOH].

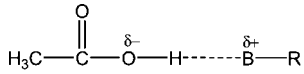

2

The free base of Ani corrected nucleophilic second-order rate constants, k_n ($= k_n^{app}/f_b$), for the nucleophilic reaction of Ani with PAn within $[AcOH]_T$ range 1.75−16.6 M in mixed AcOH−CH_3CN solvents, fit to eq 16

$$k_n = k_n^{un} + k_{ga}[AcOH]_T \qquad (16)$$

where k_n^{un} and k_{ga} represent respective uncatalyzed and general acid-catalyzed second-order and third-order rate constant for anilinolysis of PAn. The least-squares calculated values of k_n^{un} and k_{ga} for AcOH−CH_3CN solvent system are 3.39 ± 0.64 M^{-1} s^{-1} and 1.95 ± 0.06 M^{-2} s^{-1}, respectively. The observed data fit to eq 16 seems satisfactory as evident from the standard deviations associated with the calculated parameters, k_n^{un} and k_{ga}, and from maximum percent residual error of 6.0% and the plot of Figure 6a where solid line is drawn through the calculated data points.

The satisfactory fit of k_{obs} values to eq 1 as evident from the standard deviations associated with the values of calculated parameters, k_s and k_n^{app} (Table 1) as well as from the typical plots of Figures 1, 3, and 4 reveals the absence of kinetic terms $k_{gb}[Ani]^2[PAn]$ and $k_{ga}'[Ani][AniH^+][PAn]$ in the rate law. The observed rate law, rate $= k_{obs}[PAn]$, and eqs 1 and 16 can lead to eqs 17 and 18:

$$k_{obs} = k_s + (k_n^{un} + k_{ga}[AcOH]_T) f_b[Ani]_T \qquad (17)$$

$$k_n^{app} = k_n f_b \qquad (18)$$

The values of k_n, for nucleophilic reaction of Ani with PAn in mixed AcOH−THF solvent, show an almost linear increase with the increase in $[AcOH]_T$ until $[AcOH]_T \approx 14.0$ M (Figure 6b).

It may be considered that the horizontal axes of Figure 6a and b should indicate activity or molar ratio rather than $[AcOH]_T$ from the viewpoint of thermodynamics, but in solution-phase kinetics, second-order rate constants are expressed in molarity instead of activity or molar ratio. Thus, the values of k_s and k_{ga} in terms of molarity may be practically more useful. For instance, second-order rate constants for water reaction with substrates, based upon 55.5 M for pure water concentration, are used to determine the effective molarity of the analogous intramolecular reactions. The values of k_n are almost independent within $[AcOH]_T$ range 15.8−16.6 M. The values of k_n, obtained within $[AcOH]_T$ range 1.75−14.90 M, were treated with eq 16 and the least-squares calculated values of k_n^{un} and k_{ga} are -0.9 ± 0.5 M^{-1} s^{-1} and 2.69 ± 0.06 M^{-2} s^{-1}, respectively. Negative value of k_n^{un} with standard deviation of more than 50% reveals insignificant contribution of k_n^{un} compared to $k_{ga}[AcOH]_T$ in eq 16. Thus, the value of k_{ga} was also calculated from eq 16 with $k_n^{un} = 0$, and such a calculated value of k_{ga} is 2.48 ± 0.20 M^{-2} s^{-1} which is reduced by <8% compared to k_{ga} obtained from eq 16 with k_n^{un} as an unknown parameter. It is apparent from Figure 6b that all of the observed data points at $[AcOH]_T \leq 5.25$ are slightly (≤13%) negatively deviated from the predicted linearity of the plot. In order to test if these negative deviations have significant effect on the values of k_n^{un} and k_{ga}, the values of k_n, obtained within $[AcOH]_T$ range 1.75−6.13 M, were used to calculate k_n^{un} and k_{ga} from eq 16, and such respective calculated values are -0.9 ± 0.4 M^{-1} s^{-1} and 2.59 ± 0.09 M^{-2} s^{-1}. Again the negative value of k_n^{un} with standard deviation of more than 40% reveals its insignificance compared $k_{ga}[AcOH]_T$ in eq 16 with $k_n^{un} = 0$, and such a calculated value of k_{ga} is 2.32 ± 0.11 M^{-2} s^{-1}, which is ~6% lower than k_{ga} ($= 2.48$ M^{-2} s^{-1}) obtained by the use of k_n values within $[AcOH]_T$ range 1.75−14.9 M. Nearly 6% change in the magnitude of the slopes of two solid lines of Figure 6b is similar to the standard deviations associated with the values of these slopes.

SCHEME 3[a]

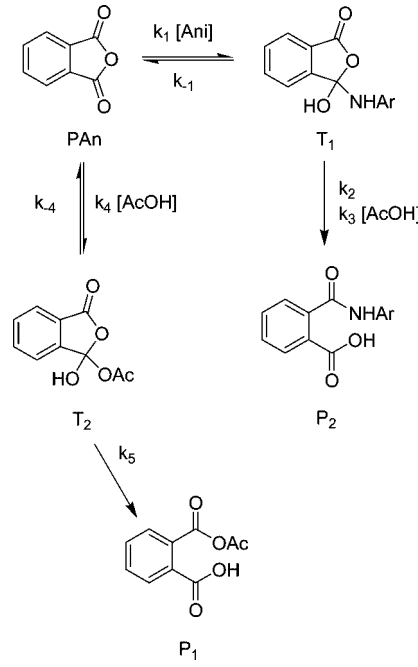

[a] An = $ArNH_2$; Ac = CH_3CO.

In view of experimental results shown by Figure 6a and b, a plausible reaction mechanism is shown in Scheme 3. Although the present data are not sufficient to support or oppose the presence of reactive intermediates T_1 and T_2 on the reaction paths, these intermediates are shown in Scheme 3 for the following reason.

The reactive intermediates T_1 and T_2 are expected to be more stable in acetic acid than in water because of the fact that intermediate **1** was detected spectrophotometrically in acetic acid, but such an intermediate could not be detected in mixed acidic aqueous−organic cosolvents.[3−6] Since the increase in the contents of protic and aprotic organic cosolvents in mixed aqueous−organic cosolvent decrease more strongly the pK_a of acidic groups of RCO_2H, $ArCO_2H$, ROH, and ArOH than those of RNH_3^+, $R_2NH_2^+$, and R_3NH^+ and therefore it is plausible to assume that the pK_a value of leaving group in the k_{-1}-step is larger than that in the k_2-step and k_3-step. Thus, based upon the better leaving ability of the leaving group in the k_{-1}-step and the release of five-membered ring strain energy in the k_2-step as well as the k_3-step, the inequality $k_{-1} \gg k_2$ and $k_{-1} \gg k_3$ [AcOH] should exist, and as a consequence the k_2-step and k_3-

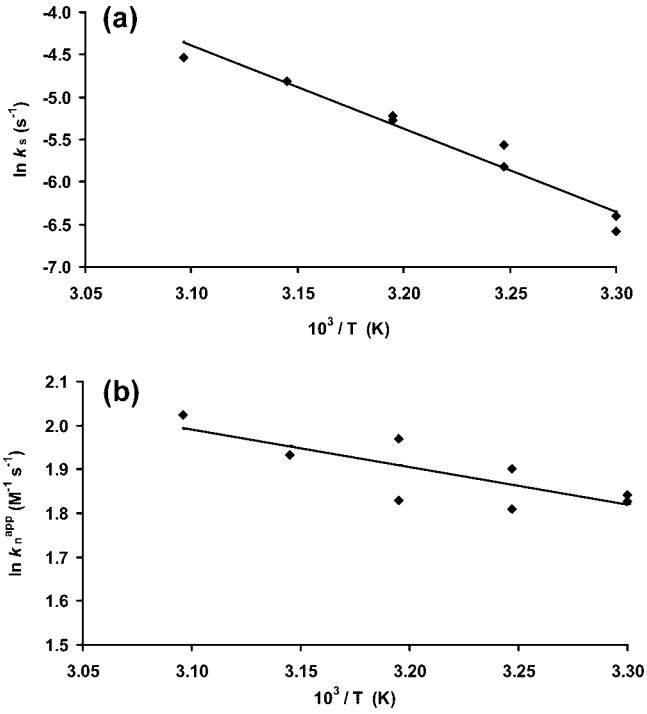

FIGURE 7. (a) Plot showing the dependence of ln k_s versus $1/T$ for acetolysis of PAn in AcOH. The solid line is drawn through the calculated data points using the Arrhenius equation with ln A and E_a mentioned in the text. (b) Plot showing the dependence of ln k_n^{app} versus $1/T$ for anilinolysis of PAn in AcOH. The solid line is drawn through the calculated data points using the Arrhenius equation with ln A and E_a mentioned in the text.

step are rate-determining steps. Similar arguments may lead to the k_4-step as the rate-determining step in the acetolysis of PAn. There is a likelihood that the k_3-step involves a transition state (TS) where the AcOH molecule acts as a bifunctional catalyst (i.e., both intermolecular general acid and general base).

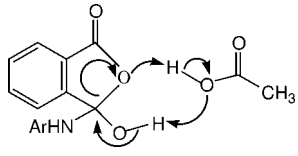

TS

Activation Parameters for Acetolysis and Anilinolysis of PAn. The rate constants k_s and k_n^{app}, obtained within the temperature range 30−50 °C at 100% v/v AcOH (Table 1), were used to calculate the activation parameters, ΔH^* and ΔS^*, from the Eyring equation as well as E_a and ln A from the Arrhenius equation. The nonlinear least-squares calculated values of activation parameters are as follows: $\Delta H^* = 15.3 \pm 1.2$ kcal mol^{-1} and $\Delta S^* = -20.1 \pm 3.8$ cal K^{-1}mol^{-1} for k_s (i.e., acetolysis of PAn) as well as $\Delta H^* = 1.1 \pm 0.5$ kcal mol^{-1} and $\Delta S^* = -51.2 \pm 1.7$ cal K^{-1}mol^{-1} for k_n^{app} (i.e., anilinolysis of PAn). Similarly, linear least-squares calculated respective values of E_a and ln A from Arrhenius equation are 19.3 ± 1.8 kcal mol^{-1} and 25.78 ± 2.87 s^{-1} for k_s as well as 1.7 ± 0.5 kcal mol^{-1} and 4.63 ± 0.87 M^{-1} s^{-1} for k_n^{app}. A satisfactory data fit to the Arrhenius equation is evident from the standard deviations associated with the calculated values of the activation parameters and from the plots of Figure 7 where solid lines are drawn through the least-squares calculated data points using the Arrhenius equation. Although the interesting finding in this paper is the unusually very low values of ΔH^* (= 1−2 kcal mol^{-1}) and ΔS^* (= −51.2 cal K^{-1}mol^{-1}) for k_n^{app}, its plausible physicochemical explanations are difficult to provide at the moment. The values of ΔH^* and ΔS^* for the hydrolysis of PAn at 0.01 M HCl are 8.6 ± 1.2 kcal mol^{-1} and -39.1 ± 3.9 cal K^{-1} mol^{-1}, respectively, and the reaction mechanism for hydrolysis under such conditions involves the presence of a reactive complex formed between PAn and water molecules.[16]

Conclusions

It is apparent from the present study that the expected maximum yield of the product (P_2) from the reaction of PAn with Ani could be obtained under the following reaction conditions: (i) The synthesis should be carried out at lower temperature because the value of k_n^{app}/k_s increases sharply with decreasing temperature at $[Ani]_T/[PAn_0] \geq 2.5$ in pure glacial acetic acid solvent. (ii) The presence of 50% v/v CH_3CN in mixed AcOH solvent should give maximum yield of P_2 within relatively shorter reaction period because the k_n^{app}/k_s value at 35 °C is larger under such condition than under pure AcOH solvent. (iii) The value of k_n^{app}/k_s at 60−70% v/v THF are significantly larger than at 50% v/v CH_3CN in mixed AcOH solvent. Thus, under such solvent system, the maximum yield of P_2 could be achieved at 35 °C within a significantly shorter reaction period compared to those under conditions of (i) and (ii).

Experimental Section

Materials. Reagent grade phthalic anhydride (PAn), aniline, glacial acetic acid (AcOH), and tetrahydrofuran (THF) were commercial products of the highest commercially available purity. HPLC grade acetonitrile was used throughout the study. AcOH was purified by distillation. Dry THF (500 mL) containing 5 g Na and 10 g benzophenone was distilled under nitrogen. *N*-Phenylphthalamic acid (P_2) was synthesized using the literature procedure involving the reaction of aniline with PAn in THF. The observed spectroscopic data are in agreement with the corresponding reported data.[2]

Kinetic Measurements. Reaction rates of the cleavage of phthalic anhydride (PAn) in glacial acetic acid (AcOH) and mixed AcOH−CH_3CN and THF−AcOH solvents containing aniline were studied spectrophotometrically by monitoring the appearance of products at 275 nm and at a constant temperature. The stock solutions of PAn (0.015 M) for kinetic runs carried out in 100% AcOH were freshly prepared just before the start of the kinetic runs. For kinetic runs, carried out in mixed AcOH−CH_3CN and THF−AcOH solvents, the stock solutions of PAn were prepared in 100% CH_3CN or THF. The details of the kinetic procedure are essentially same as described elsewhere.[17]

All kinetic runs were carried out under pseudo-first-order kinetic conditions. The observed data, absorbance (A_{ob}) versus reaction time (t) for each kinetic run were found to fit to eq 2. Pseudo-first-order rate constant (k_{obs}), apparent molar extinction coefficient (δ_{app}), and initial absorbance (A_0) were calculated from eq 2 with the nonlinear least-squares technique. The reactions were carried out for up to 6−9 half-lifes of the reactions, and the observed data fitted well to eq 2.

Product Characerization. In order to characterize the products of the cleavage of PAn in pure AcOH, and mixed AcOH−X, (X = CH_3CN, THF), solvents containing aniline, three typical kinetic

(16) Khan, M. N. *Indian J. Chem.* **1993**, *32A*, 387.
(17) Cheong, M. Y.; Ariffin, A.; Khan, M. N. *J. Phys. Chem. B* **2007**, *111*, 12185.

TABLE 4. Values of Observed Absorbance (A_{ob}^{∞}) and Estimated Absorbance (A_{ob}^{est}) of the Products of the Cleavage of PAn in pure AcOH and mixed AcOH−X, Solvents Containing Ani[a]

AcOH (% v/v)	X (% v/v)	A_{sol}	$10^{-3}\ \delta_{P1}$[b] ($M^{-1}\ cm^{-1}$)	$10^{-3}\ \delta_{P2}$[c] ($M^{-1}\ cm^{-1}$)	F_{P1}[d]	f_b[e]	A_{ob}^{∞}	A_{ob}^{est}[f]
100	0	0.03[g]	2.24	7.77	0.31	0.16	1.04[h]	1.08
100	0	0.03	2.24	7.77	0.39	0.16	1.04	1.01
50	50[i]	0.03[j]	0.41	4.72	0.06	0.37	0.90[k]	1.01
50	50	0.03	0.0	4.72	0.06	0.37	0.90	1.00
50	50	0.03	2.24	4.72	0.06	0.37	0.90	1.02
50	50[l]	0.03[m]	1.21	6.80	0.04	0.74	1.57[n]	1.63
50	50		0.0	6.80	0.04	0.74	1.57	1.62
50	50		2.24	6.80	0.04	0.74	1.57	1.64

[a] $[PAn_0] = 1.5 \times 10^{-4}$ M, $[Ani]_T = 0.001$ M, 35 °C, $\lambda = 275$ nm, and $\delta_{Ani} = 1175\ M^{-1}\ cm^{-1}$ at 275 nm. [b] $\delta_{P1} \approx \delta_{PAn} = \alpha/[PAn_0]$ with α values listed in Table 2. [c] The values of δ_{P2} were obtained by the use of authentic sample of P_2 as described in the text. [d] $F_{P1} = k_s/(k_s + k_n^{app})$ where k_s and k_n^{app} values are summarized in Table 1. [e] Values of f_b are listed in Table 1. [f] The values of A_{ob}^{est} were calculated from eq 20 as described in the text. [g] $A_{sol} = \alpha$ at 35 °C, 100% v/v AcOH, and $[PAn_0] = 0$ (Table 2). [h] The value of A_{ob}^{∞} was obtained at 7 half-lifes of the reaction. [i] X = CH_3CN. [j] $A_{sol} = \alpha = 0.01$ at 35 °C, 100% v/v CH_3CN and $[PAn_0] = 0$ (Table 2). [k] The value of A_{ob}^{∞} was obtained at 8 half-lifes of the reaction. [l] X = THF. [m] $A_{sol} = \alpha = 0.04$ at 35 °C, 100% v/v THF, and $[PAn_0] = 0$ (Table 2). [n] The value of A_{ob}^{∞} was obtained at 12 half-lifes of the reaction.

runs were carried out at 35 °C as well as 0 and 50% v/v X (X = CH_3CN, THF). The values of absorbance of these reaction mixtures (A_{ob}^{∞}) at 275 nm and reaction time $t \geq 7$ half-lifes are shown in Table 4. *N*-Phenylphthalamic acid (P_2) is known to undergo rapid cyclization to form **1** in AcOH in the absence of aniline.[2] Thus, the value of δ_{P2}, as shown in Table 4, was calculated from the A_0 value obtained from eq 2 by the use of A_{ob} versus t data (at 275 nm) of a kinetic run for the cleavage of authentic P_2 at 35 °C in pure AcOH containing 1.5×10^{-4} M P_2. In order to find out the effect of the presence of aniline (Ani) on A_0 value, another kinetic run was carried out at 35 °C in pure AcOH containing 1.5×10^{-4} M P_2 and 0.002 M Ani, and the value of A_0 was turned to be 1.51, which on applying the correction of absorption due to free Ani base ($A_{ob}^{Ani} = 0.35$) resulted in an absorbance value (A_{ob}^{P2}) due to P_2 of 1.16 which gave $\delta_{P2} = 7.73 \times 10^3\ M^{-1}\ cm^{-1}$. These observations showed the absence of any detectable effect of the presence of Ani on δ_{P2}. As described earlier in the text $\delta_{P1} \approx \delta_{PAn}$ at 275 nm in pure AcOH solvent, and as consequence, the values of δ_{P1} were obtained from α values listed in Table 2.

It is evident from Scheme 2 that the absorbance (A_{ob}^{est}) of the reaction mixture containing 1.5×10^{-4} M PAn and 1.0×10^{-3} M Ani at $t = \infty$ (i.e., t equivalent to reaction period of ≥7 half-lifes of the reactions) may be estimated from eq 19:

$$A_{ob}^{est} = A_{sol} + \delta_{P1}[P1] + \delta_{P2}[P2] + \delta_{Ani}[Ani'] \quad (19)$$

where A_{sol} represents the absorbance due to solvent, δ_Z is the molar extinction coefficient of Z (where Z = P_1, P_2, and Ani) and [Ani′] is the concentration of unreacted free Ani base. If F_{P1} and F_{P2} represent the respective fractions of product P_1 and P_2, then $F_{P1} = [P_1]/([P_1] + [P_2]) = k_s/(k_s + k_n^{app})$, $F_{P2} = 1 - F_{P1}$, and $[P_1] + [P_2] = [PAn_0]$. By introducing these defined parameters into eq 19, one gets

$$A_{ob}^{est} = A_{sol} + [PAn_0][\delta_{P1}F_{P1} + \delta_{P2}(1 - F_{P1})] + \delta_{Ani}f_b([Ani]_T - [PAn_0][2 - F_{P1}]) \quad (20)$$

where f_b represents fraction of free Ani base. The values of A_{ob}^{est} were calculated from eq 20 with the known values of A_{sol}, $[PAn_0]$, δ_{P1}, δ_{P2}, F_{P1}, δ_{Ani}, f_b, and $[Ani]_T$ as summarized in Table 4. The values of A_{ob}^{est} are almost similar to the corresponding values of A_{ob}^{∞} (Table 4) within the limits of experimental uncertainties and thus affirming P_1 and P_2 as the products of the cleavage of PAn in pure AcOH and mixed AcOH−X (X = CH_3CN, THF) solvents containing aniline.

Acknowledgment. The authors thank the Ministry of Science, Technology and Innovation for ScienceFund (Project 14-02-03-4014) and the University of Malaya for financial support. The authors also thank one of the reviewers for very extensive and constructive comments/suggestions.

Supporting Information Available: Tables I and II; Figures I and II. This material is available free of charge via the Internet at http://pubs.acs.org.

JO8011072